Available online at www.sciencedirect.com
SCIENCE DIRECT®
Chemical Physics Letters 376 (2003) 493–497
CHEMICAL PHYSICS LETTERS
www.elsevier.com/locate/cplett

Oriented nano-structured hydroxyapatite from the template

Yuanjian Zhang, Liheng Zhou, Di Li, Naicun Xue, Xiudong Xu, Jinghong Li *

State Key Laboratory of Electroanalytical Chemistry, Changchun Institute of Applied Chemistry, Chinese Academy of Sciences, Changchun 130022, China

Received 30 April 2003; in final form 18 June 2003
Published online: 9 July 2003

Abstract

Natural bone is one kind of compounds consisting of hydroxyapatite (HAp) nano-rods, which are embedded in the template of collagen matrix in vivo with the same crystallographic organization. Herein HAp nano-rods precursors were synthesized via wet chemical method. Large-scale HAp nano-wires with the same crystallographic organization as the template of anodic aluminum oxide (AAO) were obtained by the electrophoretic deposition and the technology of the template. It provides a meaningful method to study and understand the information of biological molecules' mineralization process.

1. Introduction

Hydroxyapatite (HAp, $Ca_{10}(PO_4)_6(OH)_2$) is one of the most attractive materials for bone implant due to its compositional and biological similarity to native tissues, therefore it has been extensively studied and applied in various fields [1]. Bone is an inorganic–bioorganic composite material consisting mainly of collagen proteins and HAp, and its properties depend intimately on its nano-scale structures [2,3]. Both the size and the orientation of the crystals are dictated specifically by the collagen template, and the precise structural dependence between the collagen and HAp is critical to bone's resilience and strength. Hence, it is of interest to obtain HAp nano-structures with similar crystallographic organization [4–6]. Herein we employ anodic aluminum oxide (AAO) as one template to host orientational nano-structured HAp crystalline, and attempt to provide a meaningful method to design artificial nano-structures of HAp, which can interact with and replace natural biological materials.

2. Experimental

2.1. Chemicals

$Ca(OH)_2$ (A.R), H_3PO_4 (A.R) and NaOH (A.R) were acquired from standard source and used as received. Water was purified with Milli-Q (18.2 MΩ) water system. AAO membranes (Anopore, Whatman Corporation, UK) with the

* Corresponding author. Fax: +86-431-5262243.
E-mail address: lijingh@ciac.jl.cn (J. Li).

0009-2614/03/$ - see front matter © 2003 Elsevier B.V. All rights reserved.
doi:10.1016/S0009-2614(03)01038-8

diameter of 13 mm and the pore diameter of 200 nm, as well as its porosity of 50% [7] were employed in the present study.

2.2. Synthesis

The synthesis involved two steps: (1) wet chemical synthesis of nano-scaled HAp precursors; (2) electrophoretic deposition of HAp into the pores of AAO.

In order to prepare HAp precursors, an ultrasonic treated 0.01 mol $Ca(OH)_2$ (aqueous solution) was titrated with 0.006 mol H_3PO_4. After aging, washing and filtration, the crude product was dried at 100 °C in vacuum [8,9].

HAp hosted in the pores of AAO was obtained via electrophoretic deposition [10,11]. The electrophoretic cell included the AAO as the cathode and the platinum sheet as the counter electrode, and their distance was 3.5 cm. The deposition voltage was 100 V. Suspension for the experiment was prepared by ultrasonic agitation of 0.4 g/l HAp precursors in ethanol. The extra HAp precursors absorbed on the surface of AAO were removed before characterization.

2.3. Instruments

X-ray diffraction (XRD) was recorded on RIGAKU D/max-IIB X-ray Diffractometer using Cu-Kα radiation (1.5406 Å) of 40 kV and 20 mA.

Fourier transform infrared spectroscopy was conducted at FTS135 infrared spectroscopy (Bio-Rad, USA). Transmission spectrum (FT-IR) of the HAp precursors was obtained by forming thin transparent KBr pellet containing the interesting materials. Transmission spectrum of the HAp in the pores of AAO was obtained by subtracting spectrum of HAp/AAO with that of AAO membrane (obtained directly as pellet). As AAO membrane had almost no transmission in the range of less than 995 cm^{-1}, scan range was chosen from 995 to 4000 cm^{-1}.

Electron diffraction (ED) was performed on JEOL-JEM-2010 (JEOL, Japan) electron microscopy operating at 200 kV. For ED observation, AAO was removed from HAp/AAO membrane by dissolving the AAO in 0.5 M NaOH solution and washing several times with ethanol. Samples were prepared by casting one drop of the HAp suspension onto a standard carbon-coated (200–300 Å) formvar film on copper grid (230 mesh).

Scanning electron microscopy (SEM) was performed on JEOL-JXA-840 (JEOL, Japan) electron microscopy operating at 200 kV. HAp/AAO membrane was etched in NaOH to exhibit the cross section of the HAp in the pores before SEM measurement.

X-ray photoelectron spectroscopy (XPS) was conducted using a VG ESCALAB MK II spectrometer (VG Scientific, UK) employing a monochromatic Mg-Kα X-ray source ($hv = 1253.6$ eV). Peak positions were internally referenced to the C1s peak at 284.6 eV.

3. Results and discussion

Fig. 1 shows X-ray diffraction patterns of the HAp precursors. All peaks corresponded to hexagonal HAp crystal (JCPDS 9-432) and no other calcium phosphate phases could be detected. The average crystallite size of HAp can be estimated by the Sherrer formula [9,12]

$$D_{hkl} = \frac{0.9\lambda}{\beta_{hkl}\cos\theta}. \quad (1)$$

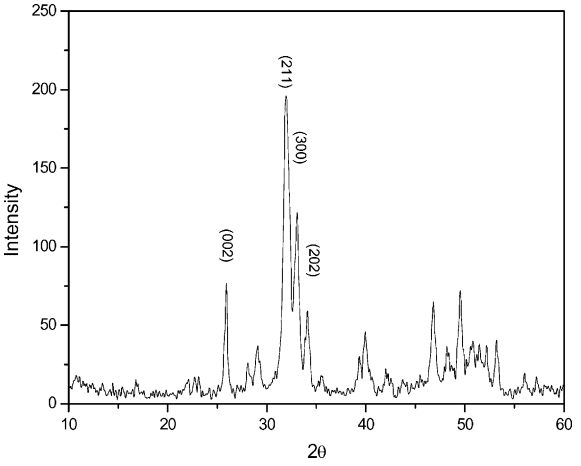

Fig. 1. XRD patterns of the HAp precursors.

The individual size of crystallite was calculated as 19.2 nm where (0 0 2) plane peak was used with $2\theta = 25.9°$. The samples were further characterized by TEM. HAp precursors were in nano-rods morphology with uniform diameters of about 6 nm and lengths of about 80 nm. Considering the average individual size of the crystallite of HAp precursors obtained by XRD observation, the HAp inclined to grow in the *c*-axis of HAp lattice [6,13].

Fig. 2 shows the morphology of the planar- and cross-section of AAO before and after electrophoretic deposition of HAp by SEM. As shown in Fig. 2a the nano-pores of AAO exhibited almost perfect two-dimension arrays with a hexagonal pattern before electrophoretic deposition. From Fig. 2b the parallel array of HAp nano-wires were observed uniformly embedded in AAO cylindrical channels with the average diameter of 190 nm and average length of 8 μm after electrophoretic deposition.

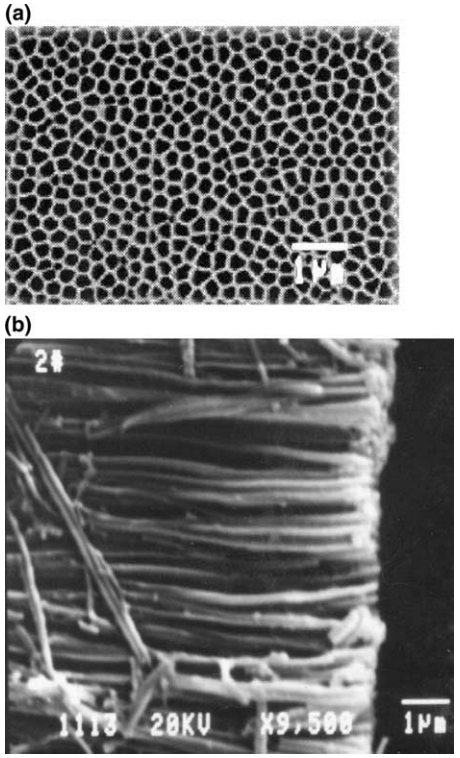

Fig. 2. SEM images of AAO membrane of the planar-section (a) and HAp/AAO of the cross-section (b).

In order to discern the relative alignment of the electrophoretic HAp nano-wires with respect to AAO pore channels, the HAp nano-wires taken from the pores of HAp/AAO membrane were characterized by electron diffraction (ED), which was demonstrated in Fig. 3. Mono-crystalline with (0 0 1) orientation of a hexagonal structure was observed [17]. The difference in the spot intensity was probably due to a slight defect in the single crystal orientation. This fact implied that the entrance of HAp precursors in AAO pores and the subsequent crystal growth were not random but were controlled by several factors such as the electrophoretic deposition condition. The exact mechanism of this control is not clear. Here we only give a possible explanation [18]. When charged HAp precursors were in an electric field, they were polarized along the direction of the electric field which co-aligned with crystal *c*-axis of HAp, and the direction of AAO pore channels also paralleled with that of the electric field. Then the rod-like HAp precursors entered the pores of AAO and were absorbed on the wall of pore channel or on other HAp along the pore channel. After that, the HAp precursors in AAO pores were re-crystallized in solid-state under the inducement of electric field.

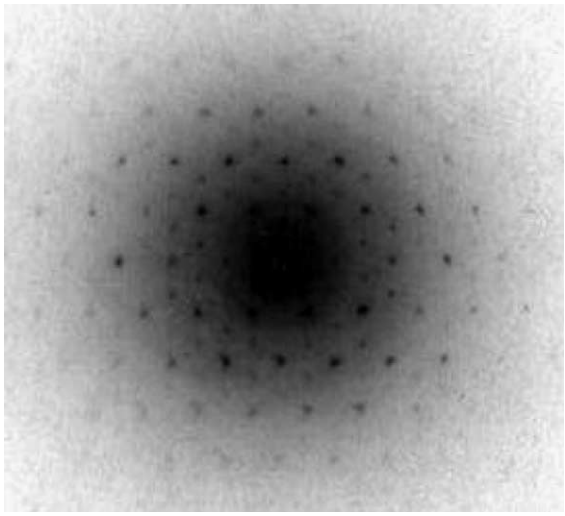

Fig. 3. ED pattern of electrophoretic nano-wires taken from the pores of HAp/AAO membrane.

Fig. 4 illustrates FT-IR spectra of the HAp precursors and HAp nano-wires in AAO, respectively. Fig. 4a shows the FT-IR spectrum of HAp precursors and their characteristic bands are indexed although other bands of the chemically adsorbed water and CO_3^{2-} were also observed [9, 12–16]. It was noticed that the characteristic bands of PO_4^{3-} near 1040 and 1100 cm^{-1}, which shown in Fig. 4b, were broadened and blue shifted when HAp precursors deposited in AAO. Moreover, interestingly, the original wide band was split into two bands notably. This phenomenon might be due to the small dimension effect and interface effect [19] of parallel HAp single crystalline nano-wires, which were aligning in the same direction of *c*-axis.

In general, the electrophoretic deposition product in the pores of AAO should be HAp [10], for only physical process could occur between HAp and Al_2O_3. XPS spectra shown in Fig. 5 further confirmed the composition of the nano-wires in the pores of AAO. The binding energy values for principal elements of HAp in the pores of AAO were in good agreement with those of HAp in literatures [20,21], which were listed in Table 1. In addition, the surface Ca/P ratio of the HAp nano-wires in pores of AAO was calculated as 1.0. Hence, the main composition of deposition product was HAp [20].

Thus, crystalline order of the HAp precursors was retained in the electrodeposited nano-wires, and large-scale HAp single crystal nano-wires with *c*-axis oriented along with the direction of the template were obtained. From the results mentioned above, it was due to several factors such as the morphology of individual HAp precursors, charged state of HAp precursors, the parallel electric field, and the special morphology of the AAO pore channels.

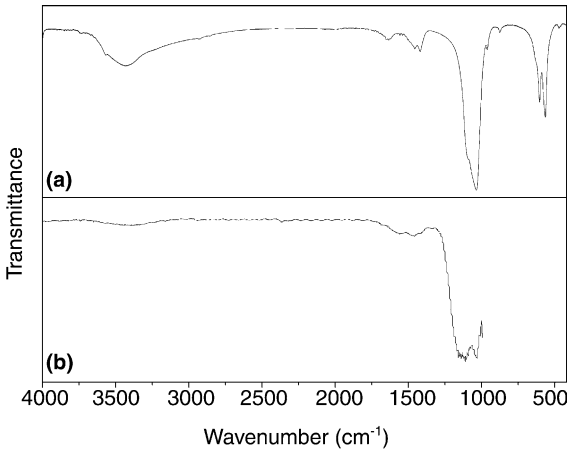

Fig. 4. FT-IR spectra of the HAp precursors (a) and the HAp nano-wires in the pores of AAO (b).

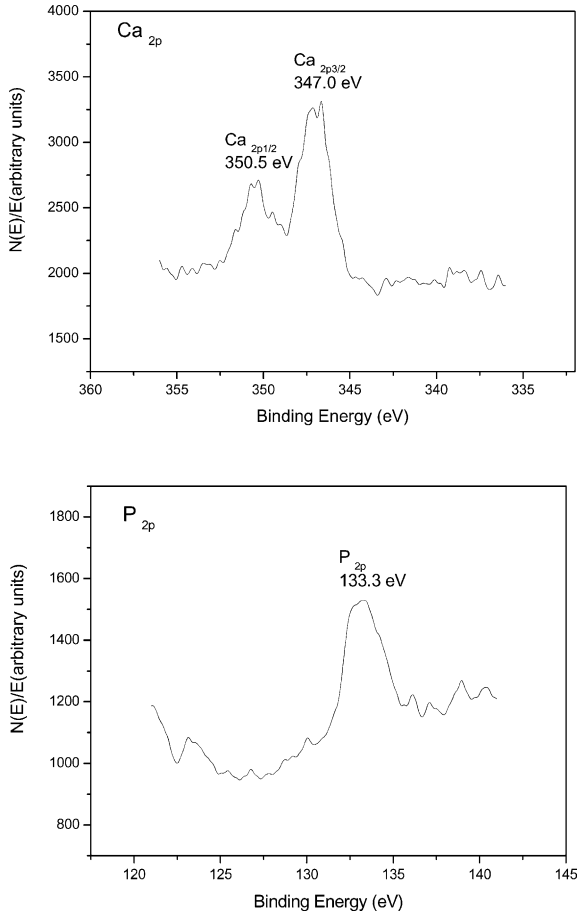

Fig. 5. XPS spectra of the HAp in the pores of AAO.

Table 1
Binding-energy values of principal elements of HAp and related samples obtained from XPS experiments

Samples	C^{1s} (eV)	$Ca^{2p3/2}$(eV)	P^{2p} (eV)
HAp/AAO	284.6	347.0	133.2
HAp [20]	286.8 ± 0.4	347.4 ± 0.2	133.9 ± 0.2
HAp [21]	285.0	347.6	133.6

In the organization of natural bone, collagen triple helices spontaneously form nano-scale bundles of protein, which act as one template and play a critical role in controlling the crystallization of HAp nano-crystals. And the *c*-axis of the HAp crystals is co-aligned with long axis of the template [4–6]. In the present experiment AAO also acted as one template to control the growth of HAp, and the HAp precursors in AAO pores were re-crystallized in solid-state after the deposition, which resulted in structural similarity to HAp found in natural bone. This organization process of HAp precursors in AAO template is similar to the mineralization process of natural bone in the template of collagen matrix. It will be helpful in the design of biomaterials, especially those used for bone tissue repair [6].

4. Conclusions

In conclusion, large-scale HAp single crystal nano-wires were synthesized via template technology, and characterized with XRD, FT-IR, TEM, SEM, ED and XPS. The results confirmed that crystalline order of the HAp precursors was retained in the electrodeposited nano-wires. The HAp single crystal nano-wires grew in *c*-axis co-orientation along with the direction of the template, which beard structural similarity to the HAp found in the natural bone. It is desired to be studied widely and thoroughly to interact with and replace natural biological materials.

Acknowledgements

This work was financially supported by Outstanding Youth Fund (No. 20125513) from the National Natural Scientific Foundation of China, 100 People Plan from Chinese Academy of Sciences and 100 Outstanding Ph.D. Thesis Award of China.

References

[1] S. Weiner, L. Addadi, J. Mater. Chem. 7 (1997) 689.
[2] S. Weiner, H.D. Wagner, Annu. Rev. Mater. Sci. 28 (1998) 271.
[3] M.D. Daniel, A.A. Ilhan, Annu. Rev. Mater. Sci. 30 (2000) 601.
[4] T.A. Taton, Nature 412 (2001) 491.
[5] R.F. Service, Science 294 (2001) 1635.
[6] J.D. Hartgerink, E. Beniash, S.I. Stupp, Science 294 (2001) 1684.
[7] The Whatman Coporation, UK. Available from http://www.whatman.com.
[8] W. Kim, F. Saito, Ultrason. Sonochem. 8 (2001) 85.
[9] L. Slavica, Z. Slavica, M. Nada, M. Slobodan, Thermochim. Acta 374 (2001) 13.
[10] I. Zhitomirsky, Mater. Lett. 42 (2000) 262.
[11] G. Hornyak, M. Kroll, R. Pugin, T. Sawitowski, G. Schmid, J. Bovin, G. Karsson, H. Hofmeister, S. Hopefe, Chem. Eur. J. 3 (1997) 1951.
[12] S. Zhang, K.E. Gonsalves, J. Mater. Sci.: Mater. Med. 8 (1997) 25.
[13] T. Furuzono, D. Walsh, K. Sato, J. Mater. Sci. Lett. 20 (2001) 111.
[14] H. Nishikawa, Mater. Lett. 50 (2001) 364.
[15] K. Hwang, J. Song, B. Kang, Y. Park, Surf. Coating Tech. 123 (2000) 252.
[16] K. Kazuhiko, Colloid Surf. B 24 (2002) 145.
[17] H.J. Kleebe, E.F. Bres, D. Bernache-Assolant, Z. Gunter, J. Am. Ceram. Soc. 80 (1997) 37.
[18] H.X. Li, M.Z. Lin, J.G. Hou, Thin Solid Films 370 (2000) 85.
[19] L.D. Zhang, J.M. Mu, Nano-Materials and Nano-Structures, Science Press of China, Beijing, 2001.
[20] S.A. Bender, J.D. Bumgardner, M.D. Roach, K. Bessho, J.L. Ong, Biomaterials 21 (2000) 299.
[21] S. Kaciulis, G. Mattogno, L. Pandolfi, M. Cavalli, G. Gnappi, A. Montenero, Appl. Surf. Sci. 151 (1999) 1.